

N71-24963
NASA CR-118317

QUARTERLY REPORT

STUDY & DETERMINATION OF AN OPTIMUM DESIGN FOR
SPACE-UTILIZED LITHIUM DOPED SOLAR CELLS

15 April 1971

13154-6019-R0-00

**CASE FILE
COPY**

Contract 952554

Jet Propulsion Laboratory
California Institute of Technology
Pasadena, California

TRW Systems Group
One Space Park
Redondo Beach, California 90278

QUARTERLY REPORT
STUDY AND DETERMINATION OF AN OPTIMUM DESIGN FOR
SPACE UTILIZED LITHIUM DOPED SOLAR CELLS

15 April 1971

13154-6019-R0-00

Prepared by:


R. G. Downing

Approved by:


A. M. Liebschutz

Contract 952554

Jet Propulsion Laboratory
California Institute of Technology
Pasadena, California

TRW Systems Group
One Space Park
Redondo Beach, California 90278

This work was performed for the Jet Propulsion Laboratory,
California Institute of Technology, as sponsored by the
National Aeronautics and Space Administration under Contract
952554.

TABLE OF CONTENTS

	<u>Page</u>
ABSTRACT	
I LITHIUM DOPED SOLAR CELL EVALUATION	1.
II KINETICS OF LITHIUM IN SILICON	6.
III PROGRESS IN THE NEXT REPORT PERIOD.	8.
IV NEW TECHNOLOGY	8.
V PAPERS AND PUBLICATIONS GENERATED	8.

LIST OF ILLUSTRATIONS

Page No.

TABLES

I	LITHIUM DIFFUSION MATRIX, C13 SERIES	9.
---	--------------------------------------	----

FIGURES

1.	DONOR CONCENTRATION (VS) DIFFUSION TIME	10.
2.	SHORT CIRCUIT CURRENT (VS) DONOR CONCENTRATION, C13A, C13B	11.
3.	SHORT CIRCUIT CURRENT (VS) DONOR CONCENTRATION, C13C, C13D	12.
4.	SHORT CIRCUIT CURRENT (VS) DONOR CONCENTRATION, C13E, C13F	13.
5.	SHORT CIRCUIT CURRENT (VS) DONOR CONCENTRATION, C13G, C13H	14.
6.	SHORT CIRCUIT CURRENT (VS) DONOR CONCENTRATION, C13I, C13J	15.
7.	DIFFUSION LENGTH (VS) ELECTRON FLUENCE	16.
8.	SHORT CIRCUIT CURRENT (VS) DIFFUSION LENGTH	17.
9.	SHORT CIRCUIT CURRENT (VS) ELECTRON FLUENCE	18.
10.	SHORT CIRCUIT CURRENT DURING RECOVERY, Q.C. CELLS	19.
11.	SHORT CIRCUIT CURRENT DURING RECOVERY, Q.C. CELLS	20.
12.	SHORT CIRCUIT CURRENT DURING RECOVERY, Q.C. CELLS	21.
13.	SHORT CIRCUIT CURRENT DURING RECOVERY, Q.C. CELLS	22.
14.	SHORT CIRCUIT CURRENT DURING RECOVERY, Q.C. CELLS	23.
15.	SHORT CIRCUIT CURRENT DURING RECOVERY, Q.C. CELLS	24.
16.	SHORT CIRCUIT CURRENT DURING RECOVERY, Q.C. CELLS	25.
17.	SHORT CIRCUIT CURRENT DURING RECOVERY, Q.C. CELLS	26.
18.	SHORT CIRCUIT CURRENT DURING RECOVERY, Q.C. CELLS	27.
19.	SHORT CIRCUIT CURRENT DURING RECOVERY, Q.C. CELLS	28.
20.	DONOR CONCENTRATION DURING RECOVERY, C13A-1	29.
21.	CHANGE IN LITHIUM DONOR CONCENTRATION DURING RECOVERY, C13A-1	30.
22.	DONOR CONCENTRATION DURING RECOVERY, C13D-1	31.
23.	CHANGE IN LITHIUM DONOR CONCENTRATION DURING RECOVERY, C13D-1	32.

ABSTRACT

A large group of lithium doped solar cells manufactured by Centralab was evaluated for radiation resistance. The cells represented a lithium diffusion time-temperature matrix. The evaluation results indicated that the higher temperature and longer diffusion time cells have undesirable variations in lithium concentration. The lithium concentrations in the cells were found to be decreasing with time in the range covered by the diffusion matrix. The relation between initial solar cell output and lithium concentration was confirmed. Capacitance-voltage techniques were used to study the changes in lithium donor concentration during the recovery period. The results indicate that previous attempts to use ion pairing to explain the recovery are inadequate. The new data indicate that radiation defects act as nuclei which allow the lithium donor to precipitate and neutralize the defect.

I LITHIUM DOPED SOLAR CELL EVALUATION

During the past quarter 100 lithium doped solar cells were received from JPL for evaluation. These cells are from the C13 series, manufactured by Centralab. The group represents a matrix of lithium diffusion temperatures and times. The matrix is designed to investigate the optimum lithium diffusion and the reproducibility of the process. All the cells were fabricated from quartz crucible grown silicon with resistivities between 25 and 40 ohm-cm. The diffusion matrix is shown in Table I. Also shown in the table are the maximum, mean, and minimum donor concentrations at the junction of the cells of each group in the matrix. The voltage-capacitance relationship or range of relationships is also shown for each group. The donor concentrations were determined by means of capacitance. Since the phosphorus concentration is approximately 1.5×10^{14} atoms/cm³, the lithium concentration can be estimated by subtracting the phosphorus concentration from the donor concentrations. Since the phosphorus concentration may go as high as 2×10^{14} atoms/cm³ (i.e., 25 ohm-cm), it can be seen that some groups in Table I may contain cells with very low lithium concentrations. Specifically these are the cells which received diffusions of 6 or 7 hours. It can also be observed that both higher temperatures and longer diffusion times result in greater variations in lithium concentration.

The mean donor concentrations of the various groups are plotted in Figure 1 as a function diffusion time. It can be seen from the data in Figure 1 that the lithium concentrations at the junction are decreasing with time, in the time span studied. Such a decreasing lithium concentration is inconsistent with diffusion from an infinite source. Since the donor concentration originally was equal to the phosphorus concentration, it was necessary for the donor concentration to rise from the original to a maximum before declining. This behavior is shown as dotted lines in Figure 1. This decrease in lithium concentration with diffusion time is characteristic of diffusion from a starved source. As the lithium source is exhausted, the surface concentration of the cells will decrease and concentrations

at the junction will decrease. In the past, manufacturers of lithium solar cells have interrupted the lithium diffusion and removed the lithium source to produce starved source diffusion. This second diffusion has been referred to as a redistribution. The data in Figure 1 indicates that redistribution is not necessary. It is not clear what causes the exhaustion of the lithium source.

The before irradiation I-V characteristics of the C13 series cells were measured under tungsten illumination. The short circuit currents of these cells were analyzed in relation to the lithium concentration. These data are shown in Figures 2 through 6. In these figures, the short circuit current of the cell is plotted versus the donor concentration at the junction. The data for groups C13A and C13B are shown in Figure 2. In this case, there is very little variation of the lithium concentration and the I_{sc} values fall in a fairly close grouping between 60 and 66 ma for the two square cm cells. In this case the I_{sc} variation appears to be a result of variations in the recombination center concentrations present after manufacture.

In Figure 3, the results for Groups C13C and C13D are shown. These cells show a tendency for the short circuit current to decrease with increasing donor concentration. In Figures 4 through 6, the tendency for I_{sc} to decrease with higher donor concentrations becomes a clear trend. The cell groups shown in Figures 4 through 6 are those diffused at the higher temperatures (350°C, 360°C, and 370°C). It would appear that the suggested relationship is a valid one, but the wider variations in lithium concentration caused by higher temperature diffusions are necessary to observe the behavior.

The nature of the degradation process in solar cells is such that the minority carrier diffusion length of the cell is reduced as the reciprocal of the square root of the damaging particle fluence. This relationship assumes only that the damage sites are created linearly with increasing particle fluence and that all sites formed are retained during further irradiation. It also must be assumed that all damage sites of the same

species which are generated will be equally effective. This means changes in the fill factor will not occur and changes in injection level are not produced by the irradiation. Despite these restrictions, it is found that the behavior of conventional solar cells is consistent with above description. This behavior is illustrated by the dashed lines shown on Figure 7. Two lithium doped p/n cells were irradiated to a total fluence of $3 \times 10^{15} \text{ e/cm}^2$. The manner in which their diffusion length decreased with electron fluence is also shown in Figure 7. It is apparent that the lithium cells do not behave in the manner of conventional cells, because the slope of their degradation curves are significantly lower than those of the conventional cells.

This point is of particular interest in the determination of damage coefficients. The expression for the damage coefficient is:

$$\frac{1}{L^2} = \frac{1}{L_0^2} + K \Phi$$

where

L = diffusion coefficient after irradiation

L_0 = diffusion coefficient before irradiation

Φ = electron fluence

K = the damage coefficient

The damage coefficient is meaningful only if the L and Φ relationship has a $-1/2$ slope, as shown by conventional cells. Since the lithium doped cells have lower slopes, the calculated K values will be functions of the electron fluence rather than constants. Since this quantity is often used to compare the radiation hardness of solar cells, it would appear its value in lithium doped cell evaluations would be limited.

Because of the manner in which solar cells operate, one empirically finds a direct relation between short circuit current and logarithm of the measured minority carrier diffusion length. We have verified this relationship, and the usual trend for high efficiency conventional cells

is shown in Figure 8. The experimental data accumulated from two lithium doped cells is also shown in Figure 9. It is obvious that the relationship for lithium doped cells is significantly different from conventional cells. The most puzzling aspect of the difference is the high short circuit currents developed by the lithium doped cells despite their relatively low minority carrier diffusion length. Cell C13D-1 is able to generate a I_{sc} of 63 ma despite the fact that its diffusion length was only 60 μm . The explanation of this effect is not clear at this time. As a result of the non-linear behavior shown in Figure 7, the changes of short circuit current observed for lithium doped cells during irradiation differ from those in conventional solar cells. Our extensive studies in the past have established a consistent relationship between degraded short circuit current and electron fluence. It has always been found that cells degrade in I_{sc} by 6.5 ma/cm² decade fluence. The rate has been found for all types of irradiation with all types of penetrating radiation. It can be seen from the data in Figure 9 that the lithium doped cells degrade at a different rate than conventional. One possible cause of this behavior could be that some annealing of defects may occur during the irradiation of the lithium doped cells. Further work is necessary to verify this explanation.

Three cells of each C13 series group were irradiated with $3 \times 10^{15} \text{ e/cm}^2$ (1 MeV) and were allowed to recover at 60°C. The most pronounced changes during recovery occur to the short circuit current. The open circuit voltages of nearly all cells in the C13 series were about 0.6V. After a $3 \times 10^{15} \text{ e/cm}^2$ irradiation, the V_{oc} was reduced to about 0.45 in all cases. Very little recovery is subsequently observed in this parameter. The changes in I_{sc} for cells of the C13 series are shown in Figures 10 through 19. Several general observations can be made about these cells. With a few exceptions, the $3 \times 10^{15} \text{ e/cm}^2$ irradiation reduced the I_{sc} to 20 to 25 ma. In most cases, the time necessary for the I_{sc} to reach the half recovery point was 100 to 200 hours at 60°C. This time is somewhat longer than what was previously found in similar cells. Except for cells with low lithium concentration, most cells ultimately recover to I_{sc} values of 35 - 38 ma. The most important factor in the extent of the recovery is the lithium concentration at the

junction rather than the diffusion schedule. As previously noted, the shorter, low temperature diffusions produce the more consistent results. The donor concentration of each cell irradiated is noted on the respective figures. The lithium concentration at the junction can be determined by subtracting the approximate phosphorus concentration ($1.5 \times 10^{14}/\text{cm}^3$) from the donor concentration.

II KINETICS OF LITHIUM IN SILICON

In our previous work we made several studies of the carrier removal in lithium doped solar cells during irradiation. This information was of considerable use in the formulation of models to describe damage process. As more information is accumulated, it is obvious that the original model proposed to describe the recovery process requires modification. The original models proposed involved the pairing of a single mobile lithium donor with a radiation-generated recombination center. Although some assumptions are necessary, the data suggest that the concentration of lithium reacting during the recovery period is much greater than the concentration of recombination centers produced by fast electrons. For this reason, systematic studies were made of the capacitance changes which occur during the recovery period of cells made from quartz crucible silicon.

Using previously described capacitance versus voltage methods¹, the donor concentrations at various distances into the n-type base were determined before and after irradiation and during the recovery process. The results of such a study of Cell C13A-1 are shown in Figure 20. After 720 hours the recovery process, as indicated by the I_{sc} is nearly complete and the changes in donor concentration have diminished. To allow a more systematic study of the lithium donor changes, the data for specific barrier widths were reduced to lithium donor concentration and normalized to that present immediately after an irradiation with 3×10^{15} e/cm². These data are shown as a function of time after irradiation, at three different points in the cell, in Figure 21.

The mathematical form of the change in lithium concentration with time could indicate information regarding the nature of the recovery process. The data in Figure 21 are plotted in semilog form to detect any relationship between the logarithm of the lithium concentration and the time elapsed. Such relationships may indicate first order chemical kinetics or some aspects of the precipitation of a second phase. The data in Figure 21 indicate that the lithium concentration decreases in a nearly straight line form until half of the lithium donors have reacted. The rate of

reaction appears to slow to zero as the lithium concentration approaches about 25% of its original value. A similar analysis was made on Cell C13D-1 after an irradiation of $3 \times 10^{15} \text{ e/cm}^2$. These results are shown in Figures 22 and 23. Although the lithium concentrations in Cell C13D-1 are higher than those in Cell C13A-1, the results are very similar. The linearity of lithium decrease during the first portion of the decline could not be confirmed because the reaction proceeded more rapidly.

It was established earlier that an irradiation of $3 \times 10^{15} \text{ e/cm}^2$ produced a uniform concentration of defects (probably Si-A centers) of 6×10^{14} in a lithium doped cell made from quartz crucible silicon.² Our recent work has indicated that such an irradiation will cause at least 70% of lithium present to react with the defects.¹ Using Cell C13D-1 as an example, this means that near the zero bias position of the n-type side of the space charge region ($2 \mu\text{m}$) about $6 \times 10^{14} \text{ cm}^{-3}$ lithium donors react during the recovery. This amounts to a one to one relation between defects and reacting lithium donors. At a distance of $3 \mu\text{m}$ deeper in the n-type region, about $3 \times 10^{15} \text{ cm}^{-3}$ lithium donors react during recovery. At this point, the concentration of lithium donors reacting during the recovery period is 5 times that of the radiation defects detected. It would be highly desirable to extend these measurements to deeper areas of the n-type base. After the $3 \times 10^{15} \text{ e/cm}^2$ irradiation of Cell C13D-1, the measured diffusion length of the cell was $4.3 \mu\text{m}$. The data in Figure 22 indicate that immediately after the irradiation, the capacitance - voltage measurement investigates the lithium concentration of the entire active portion of the n-type base. During the recovery phase, the measured diffusion length increased to $17.5 \mu\text{m}$. The distance is currently beyond the limits of the capacitance technique. If the original concentration of donors found before irradiation is extrapolated to $17.5 \mu\text{m}$, about $2 \times 10^{16} \text{ cm}^{-3}$ lithium donors are present. If 75% of these react during recovery phase, 50 lithium donor ion cores react for each radiation defect detected. Such behavior is clearly beyond explanation by models previously proposed. A model involving the nucleation of lithium precipitation by the radiation defects appears to be the only one consistent with observed results.

1 TRW Interim Final Report, Contract 952554, 19 June 1970

2 TRW Quarterly Report, Contract 952554, 15 Jan. 1971

III PROGRESS PLANNED IN THE NEXT REPORTING PERIOD

During the next reporting period the irradiation of JPL-furnished solar cells will be continued. Capacitance measurements made on cells irradiated will be analyzed to allow a thorough study of the lithium concentration changes which occur during irradiation and recovery. The study of p-type lithium counterdoped devices will be continued to investigate possible radiation hardness benefits.

IV NEW TECHNOLOGY

There is no new technology reported in this paper.

V PAPERS AND PUBLICATIONS GENERATED

Presented

Title: "Role of Lithium in Irradiated Solar Cells"

Meeting: International Colloquium on Solar Cells, Toulouse, France, 6 July 1970.

Title: "Role of Lithium in Irradiated Solar Cell Behavior"

Meeting: Eight Photovoltaic Specialists Conference, Seattle, Washington, 11 August 1970.

Submitted

Title: "Role of Lithium in Irradiated Solar Cell Behavior"

Journal: Energy Conversion

Published

Title: "Effect of Electron Irradiation on Lithium Doped Silicon"

Journal: International Journal of Physics and Chemistry of Solids Vol. 31, p. 2405, 1970

Time Temperature	3 Hrs.	4 Hrs.	5 Hrs.	6 Hrs.	7 Hrs.
330°C		<u>C13A</u> 4.6×10^{14} 4.0×10^{14} 3.4×10^{14} $k = VC^{3.4}$		<u>C13B</u> 4.2×10^{14} 3.1×10^{14} 2.4×10^{14} $k = VC^{3.5}$	
340°C	<u>C13C</u> 5.2×10^{14} 4.8×10^{14} 4.0×10^{14} $k = VC^{3.6}$				<u>C13D</u> 5.6×10^{14} 3.6×10^{14} 1.8×10^{14} $k = VC^{3.2}, k = VC^{3.7}$
350°C			<u>C13E</u> 6.2×10^{14} 4.65×10^{14} 2.9×10^{14} $k = VC^{3.5}, k = VC^{3.74}$ <u>C13F</u> 6.1×10^{14} 4.81×10^{14} 3.4×10^{14} $k = VC^{3.3}, k = VC^{3.7}$		
360°C	<u>C13G</u> 7.8×10^{14} 6.5×10^{14} 5.1×10^{14} $k = VC^{3.6}, k = VC^{3.7}$				<u>C13H</u> 5.8×10^{14} 3.7×10^{14} 2.1×10^{14} $k = VC^{2.9}, k = VC^{3.6}$
370°C		<u>C13I</u> 7.5×10^{14} 5.8×10^{14} 3.2×10^{14} $k = VC^{3.2}, k = VC^{3.8}$		<u>C13J</u> 4.4×10^{14} 3.2×10^{14} 2.2×10^{14} $k = VC^{2.9}, k = VC^{3.3}$	

Table I. Lithium Diffusion Matrix C13 Series; Maximum, Mean and Minimum Donor Concentration at Junction; Voltage - Capacitance Relationship

Table 1. Lithium Diffusion Matrix, C13 Series

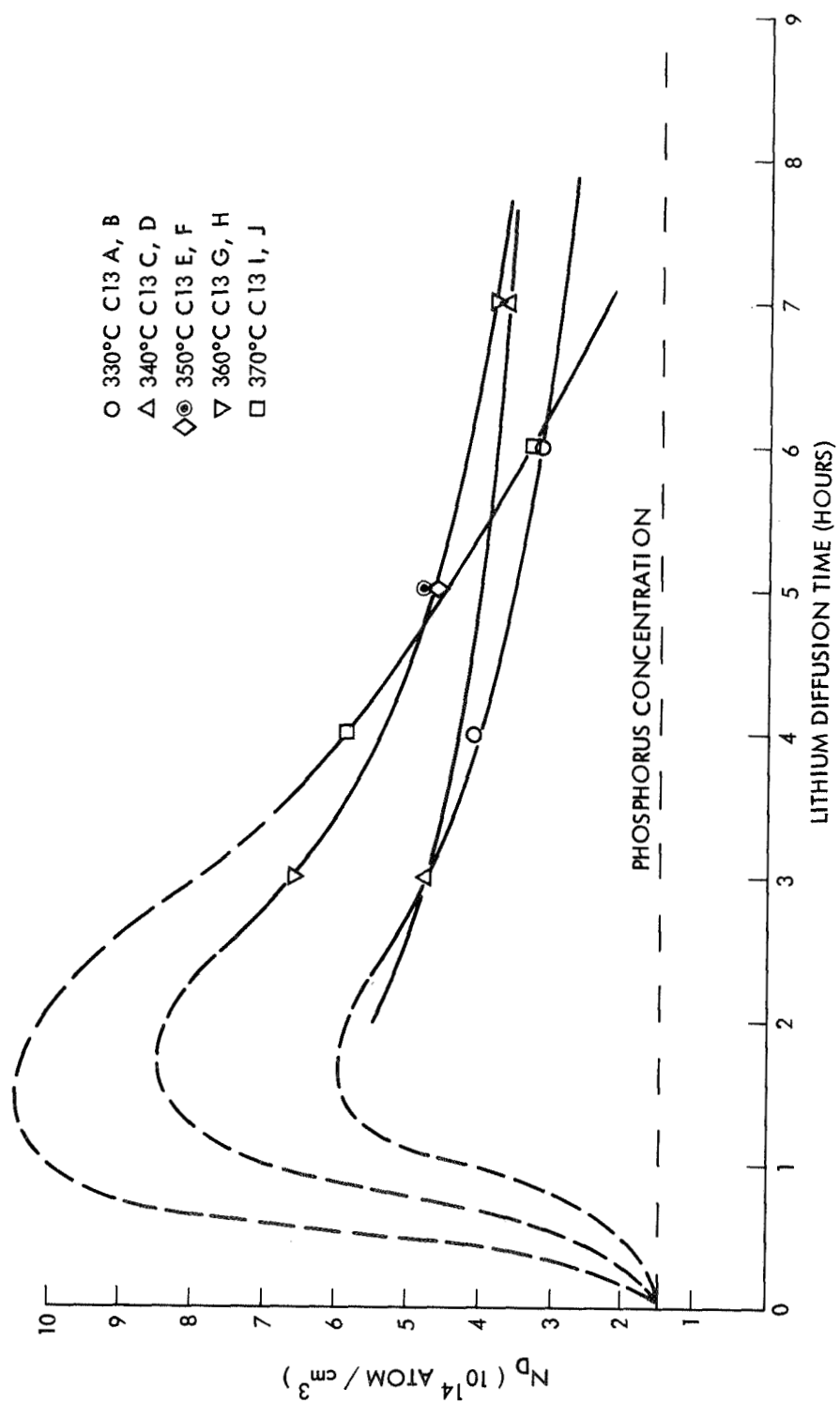


Figure 1. Donor Concentration (vs) Diffusion Time

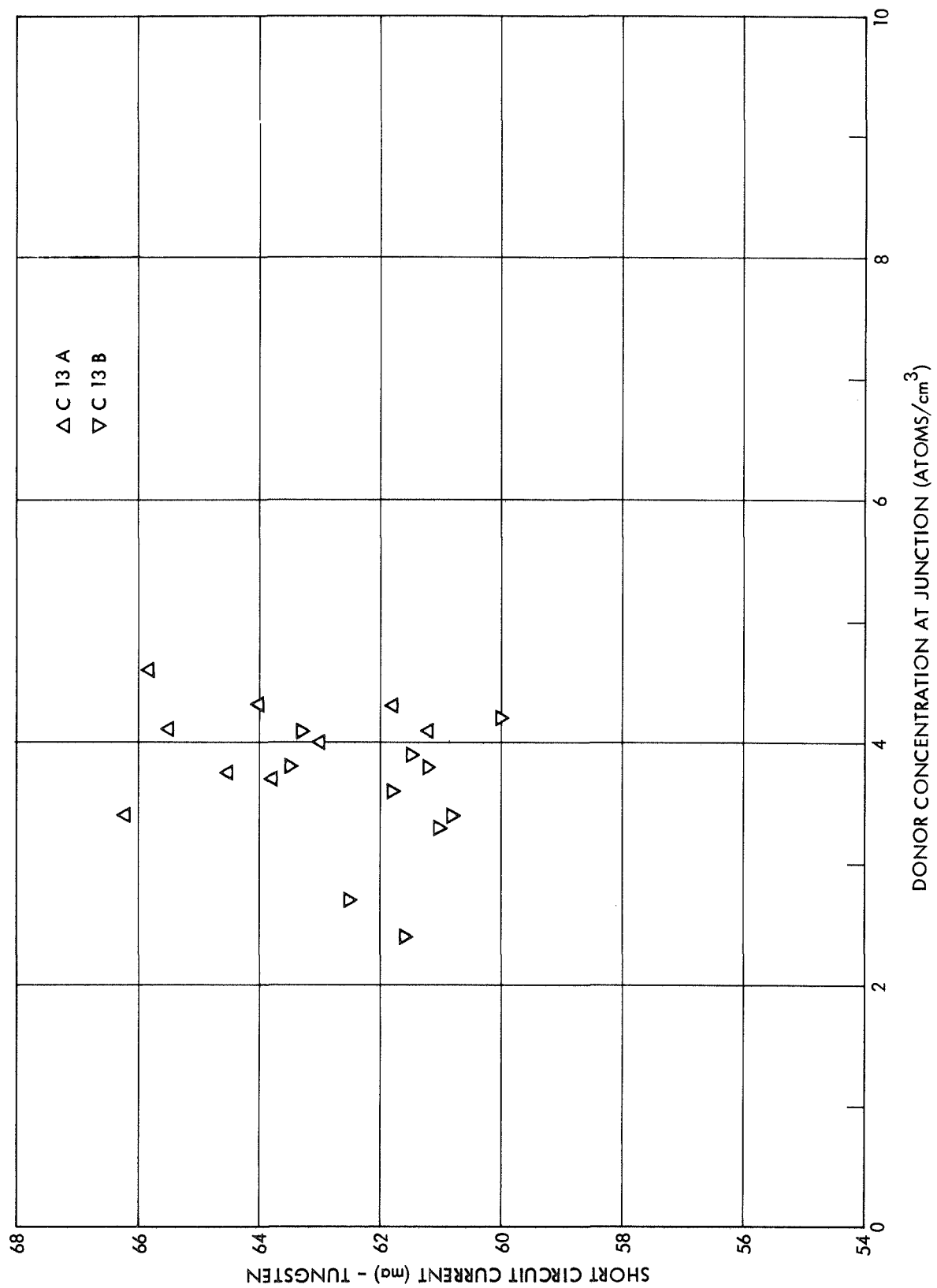


Figure 2. Short Circuit Current (vs) Donor Concentration, C13A, C13B.

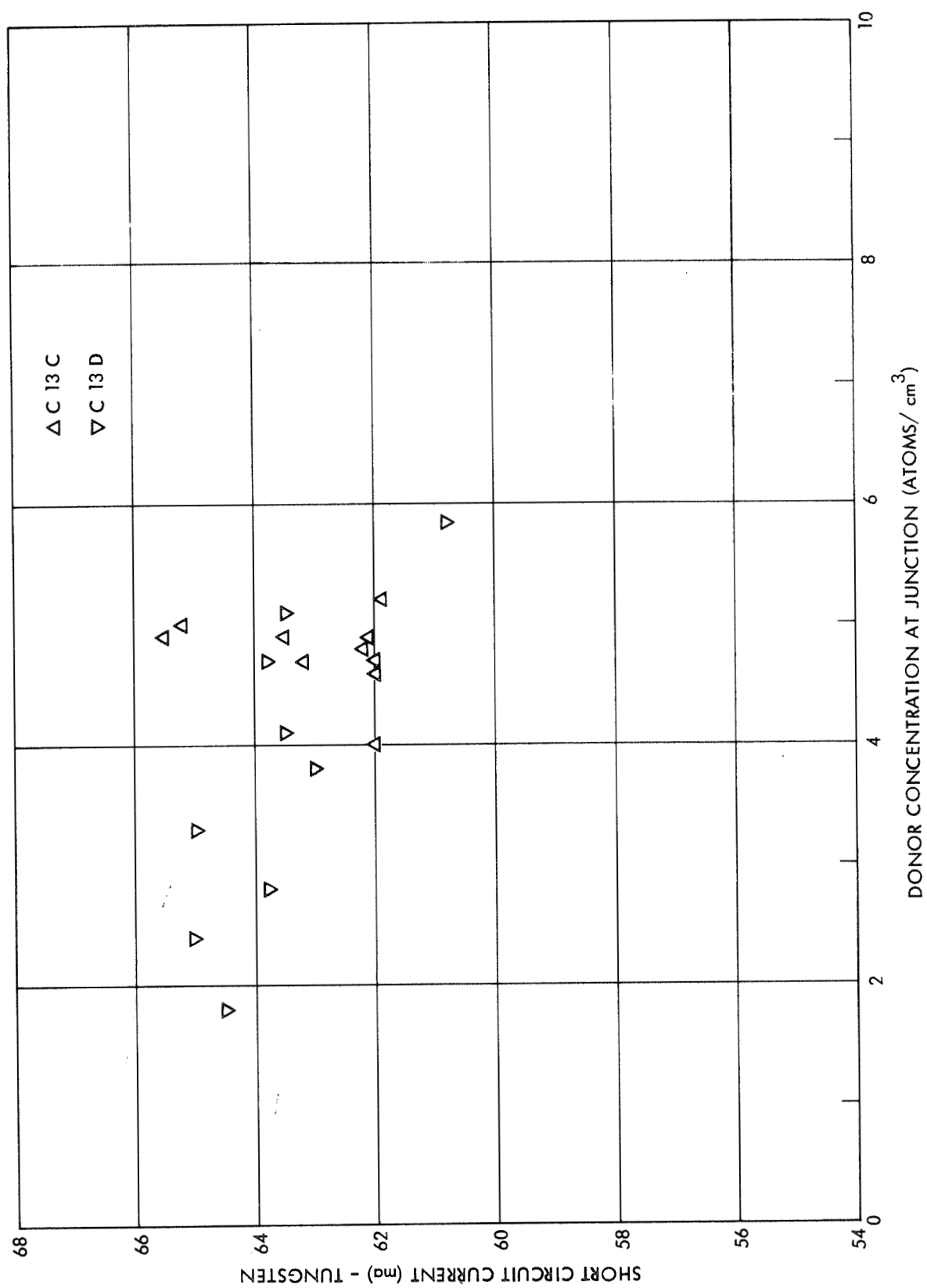


Figure 3. Short Circuit Current (vs) Donor Concentration, C13C, C13D.

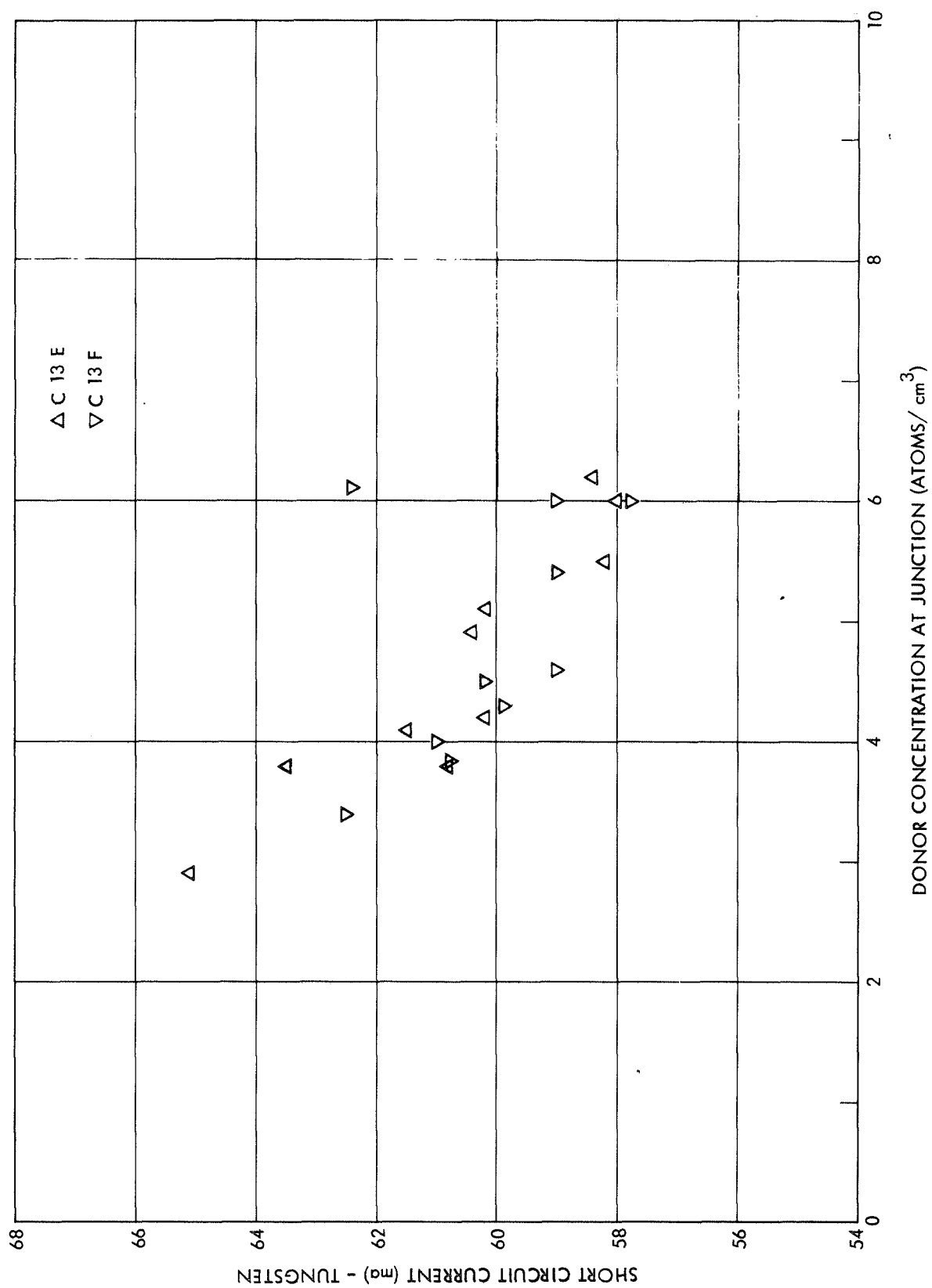


Figure 4. Short Circuit Current (vs) Donor Concentration, C13E, C13F

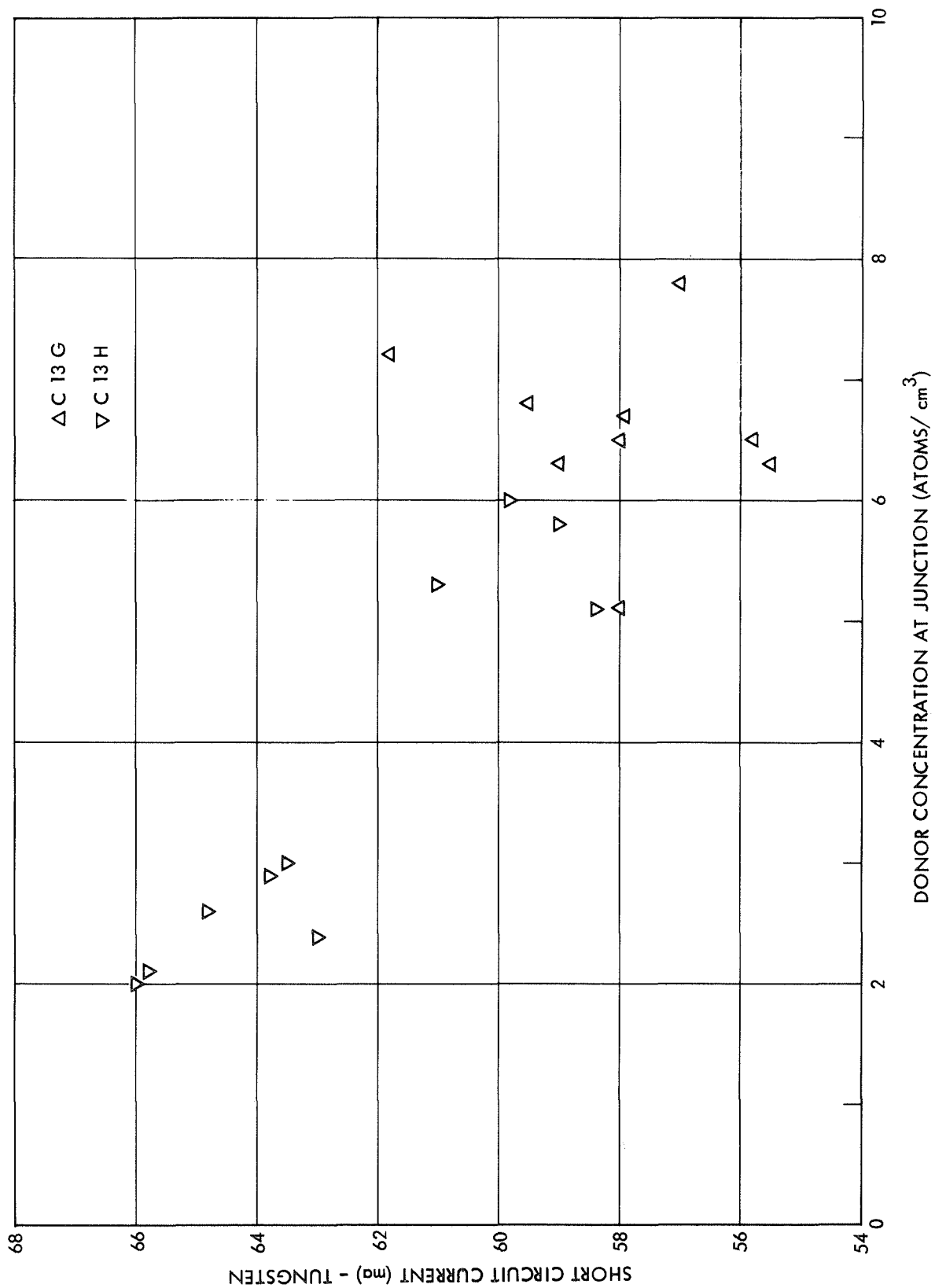


Figure 5. Short Circuit Current (vs) Donor Concentration, C13G, C13H.

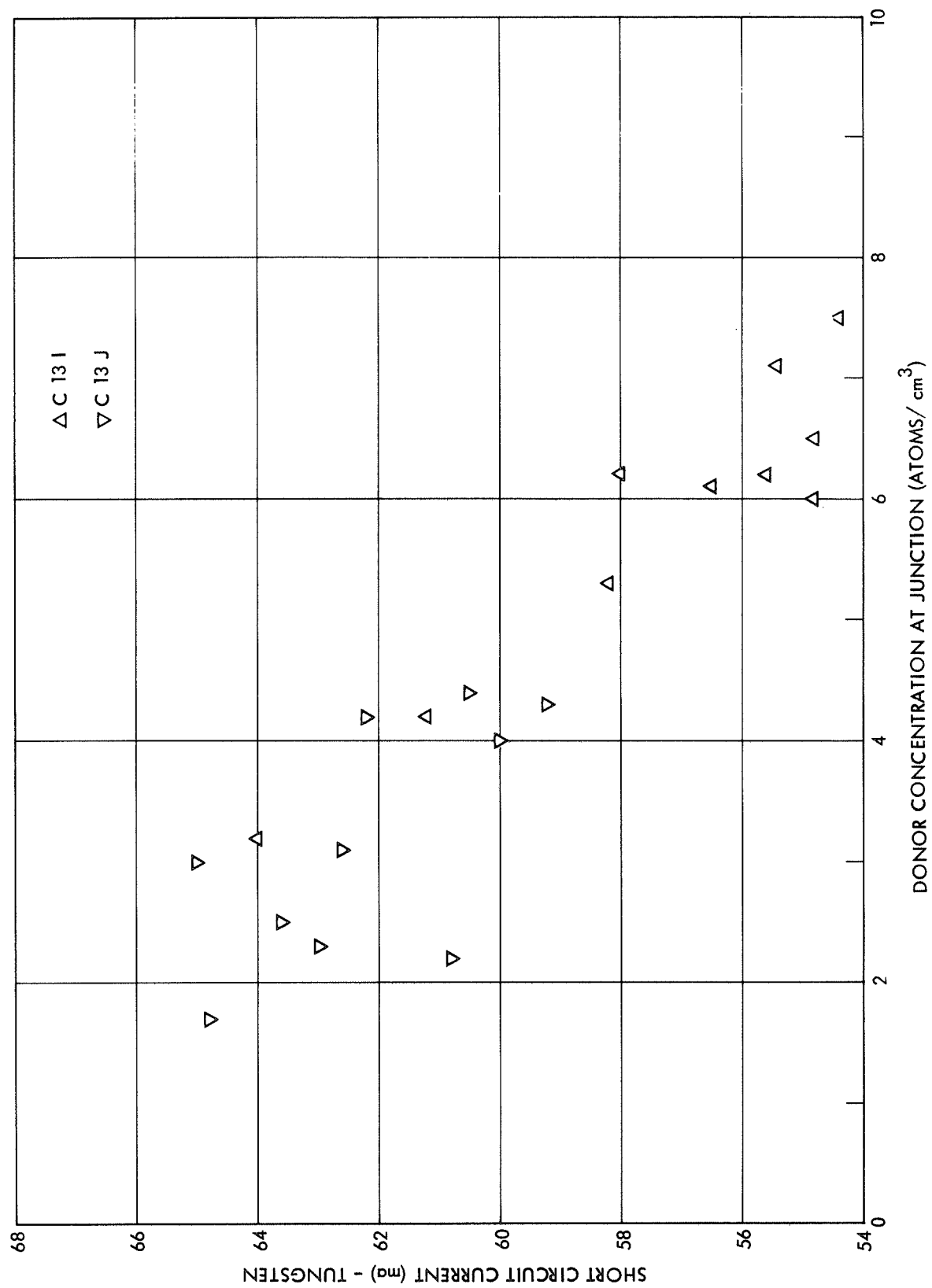


Figure 6. Short Circuit Current (vs) Donor Concentration, C13I, C13J.

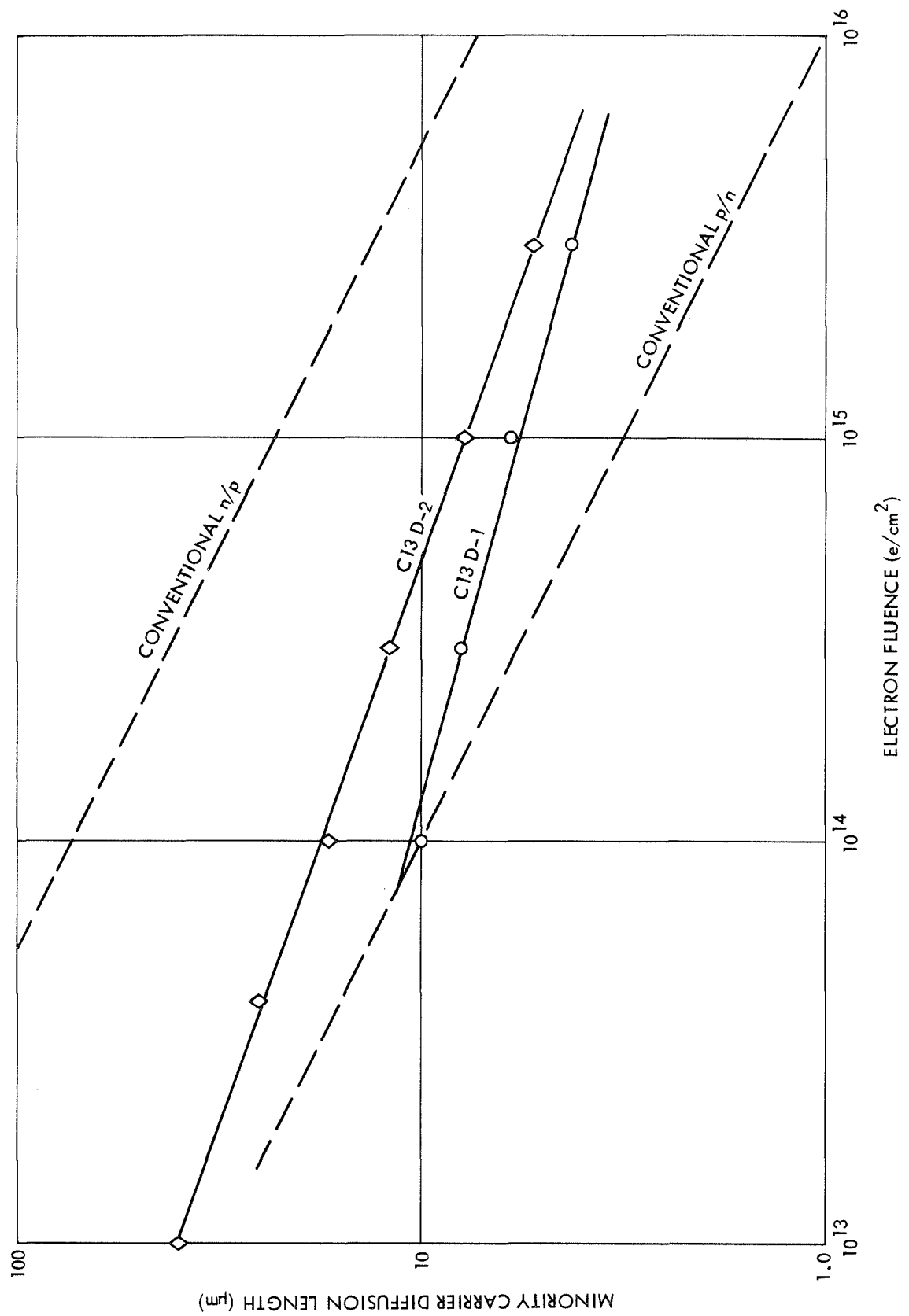


Figure 7. Diffusion Length (vs) Electron Fluence

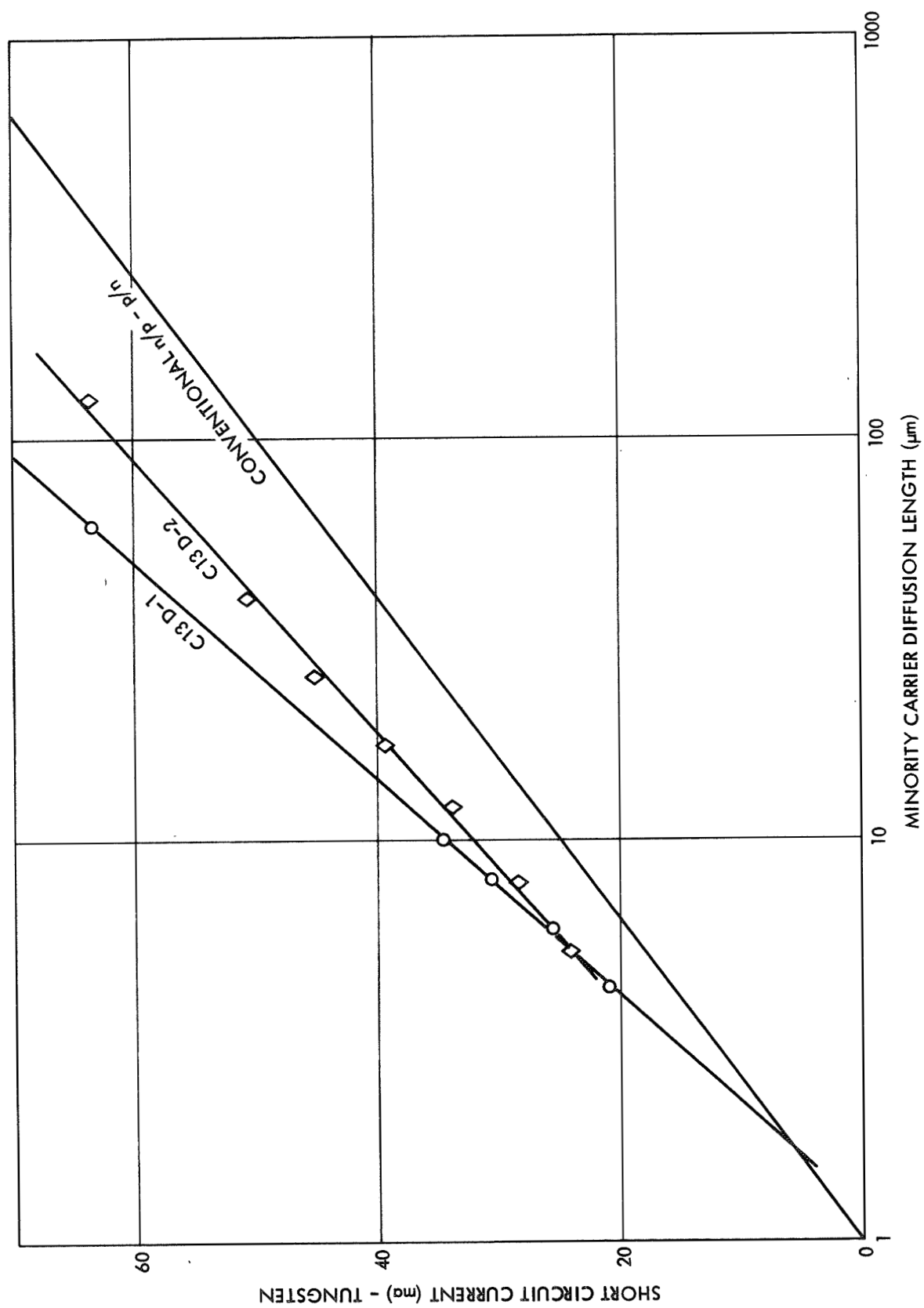


Figure 8. Short Circuit Current (vs) Diffusion Length

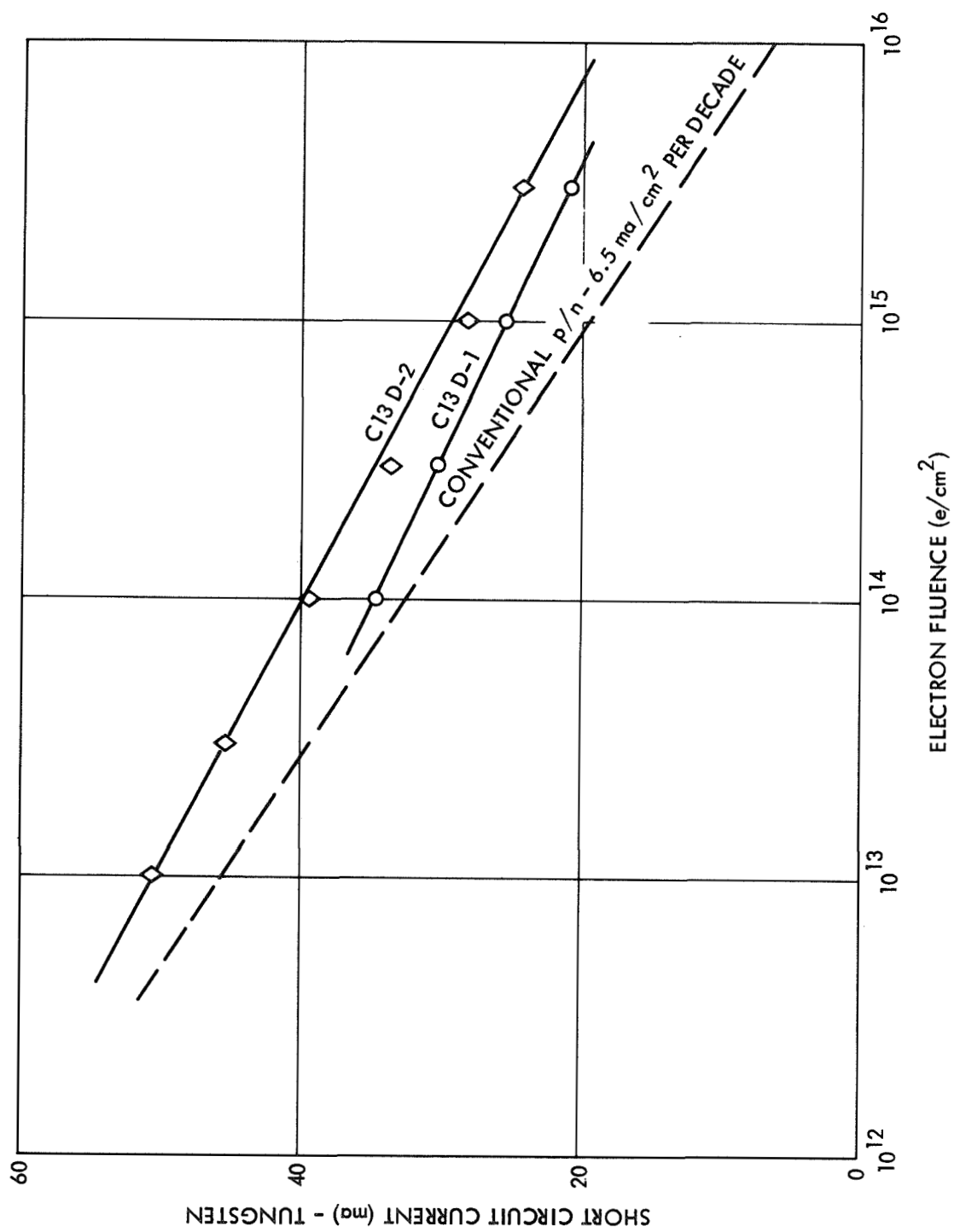
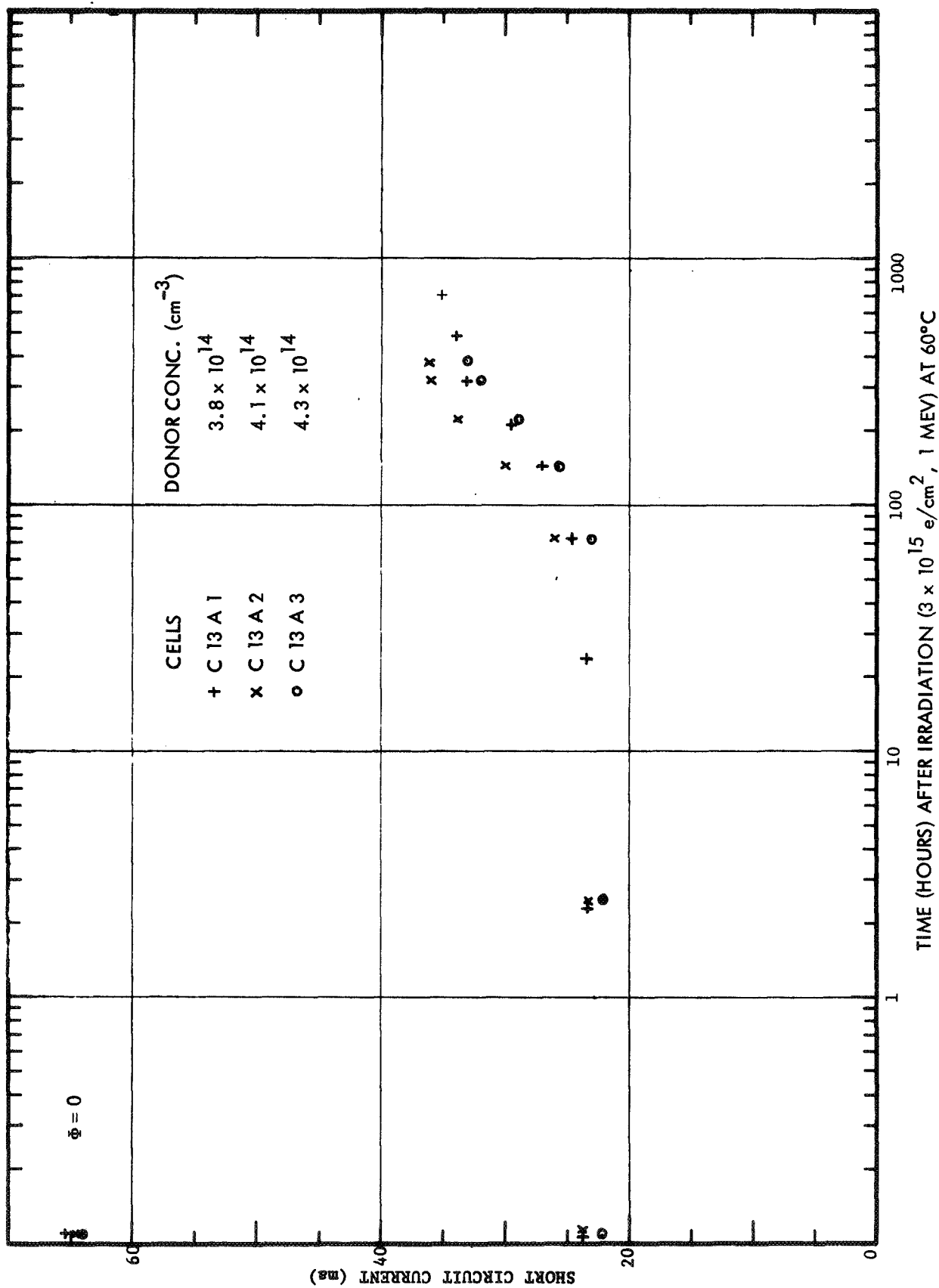


Figure 9. Short Circuit Current (vs) Electron Fluence



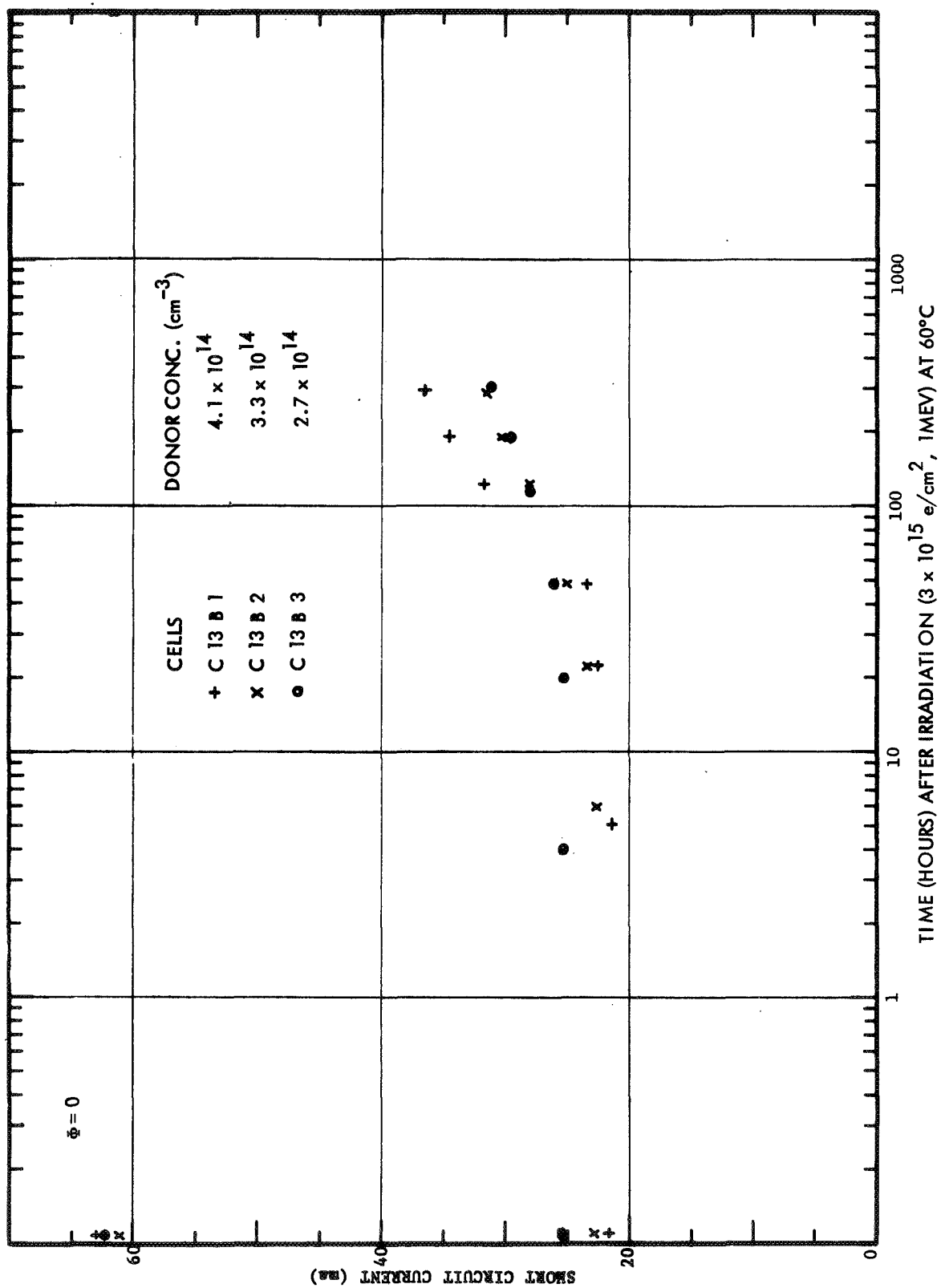


Figure 11. Short Circuit Current During Recovery, Q.C. Cell

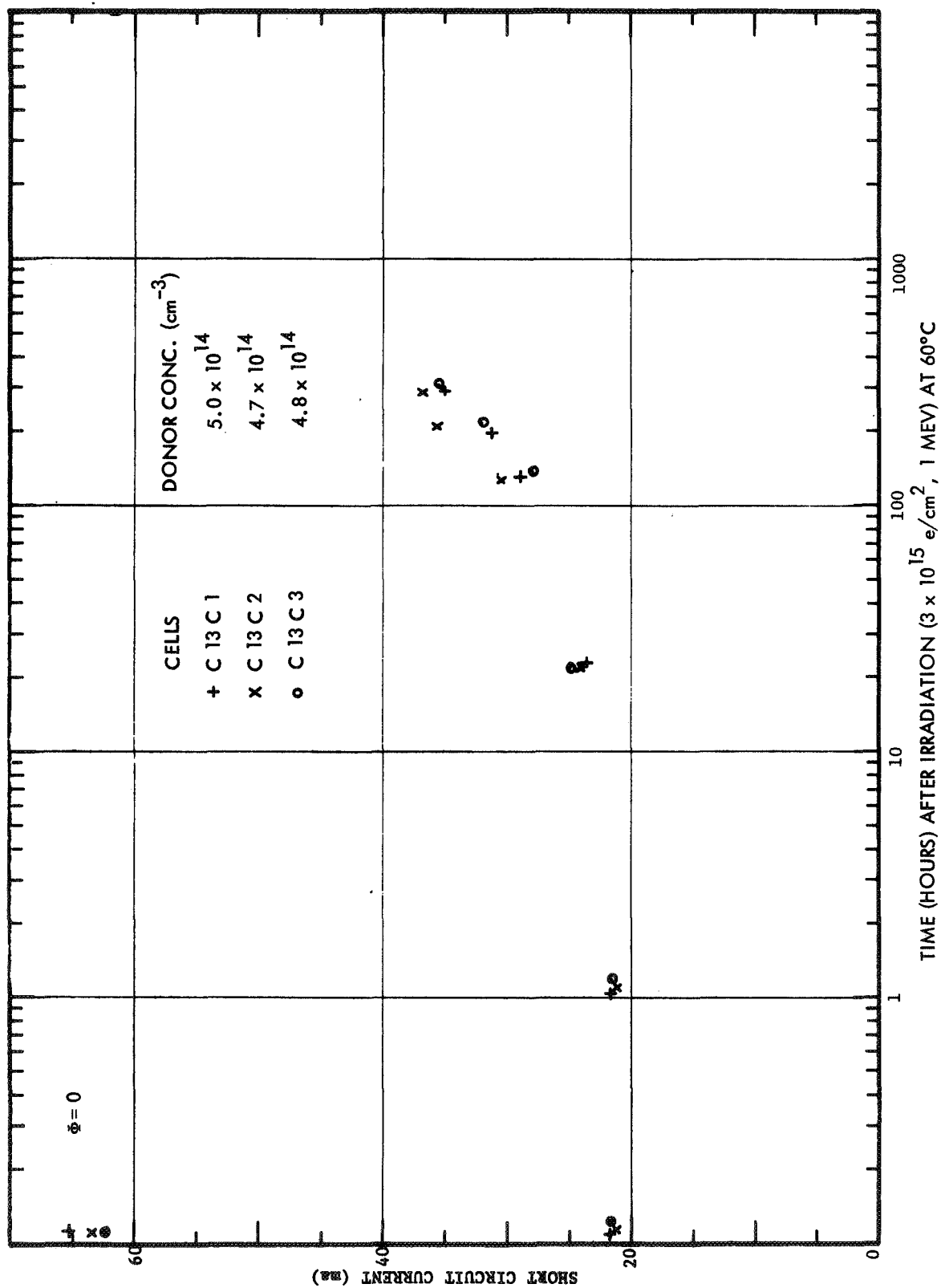


Figure 12. Short Circuit Current During Recovery, Q.C. Cell

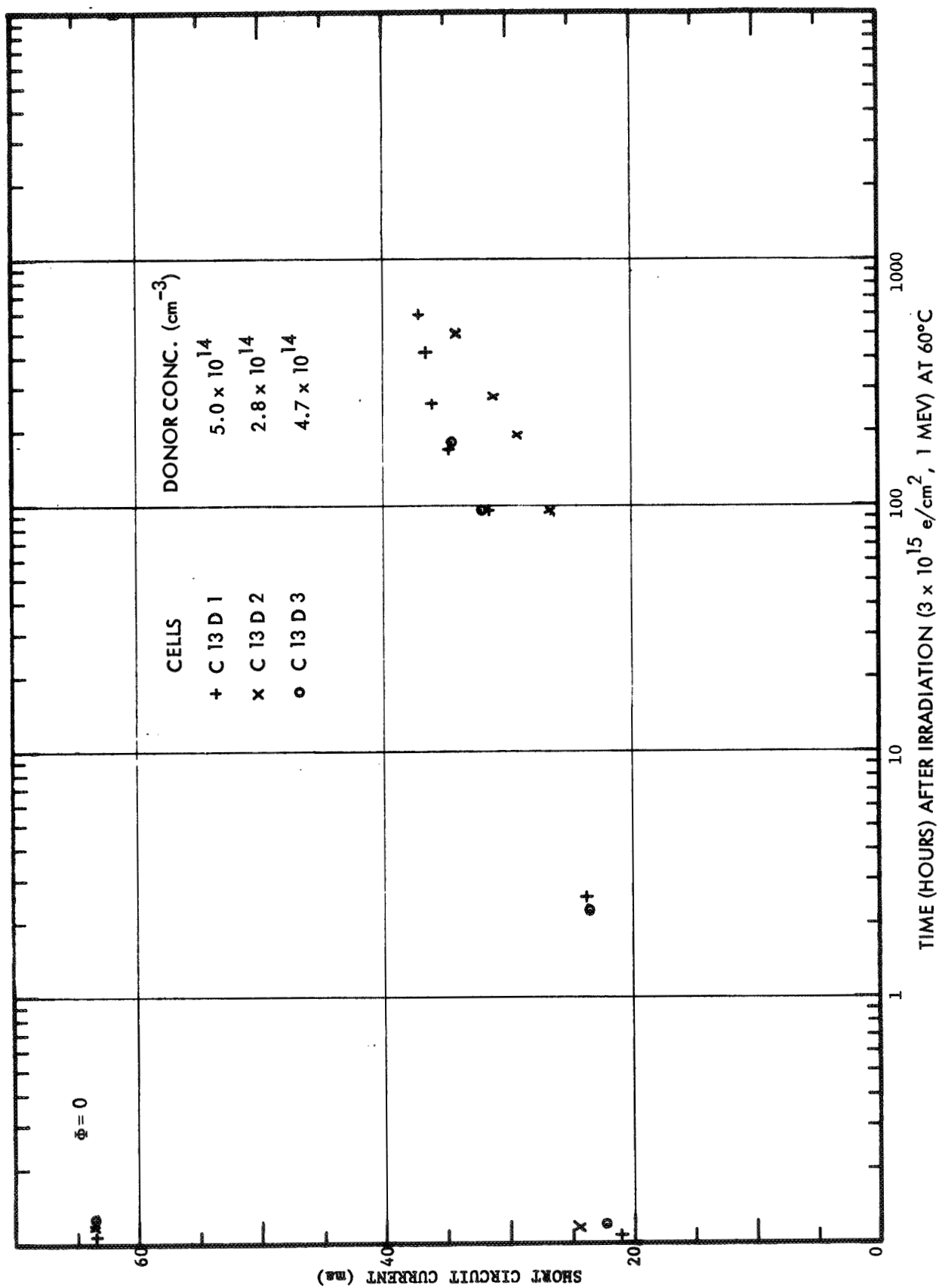


Figure 13. Short Circuit Current During Recovery, Q.C. Cell

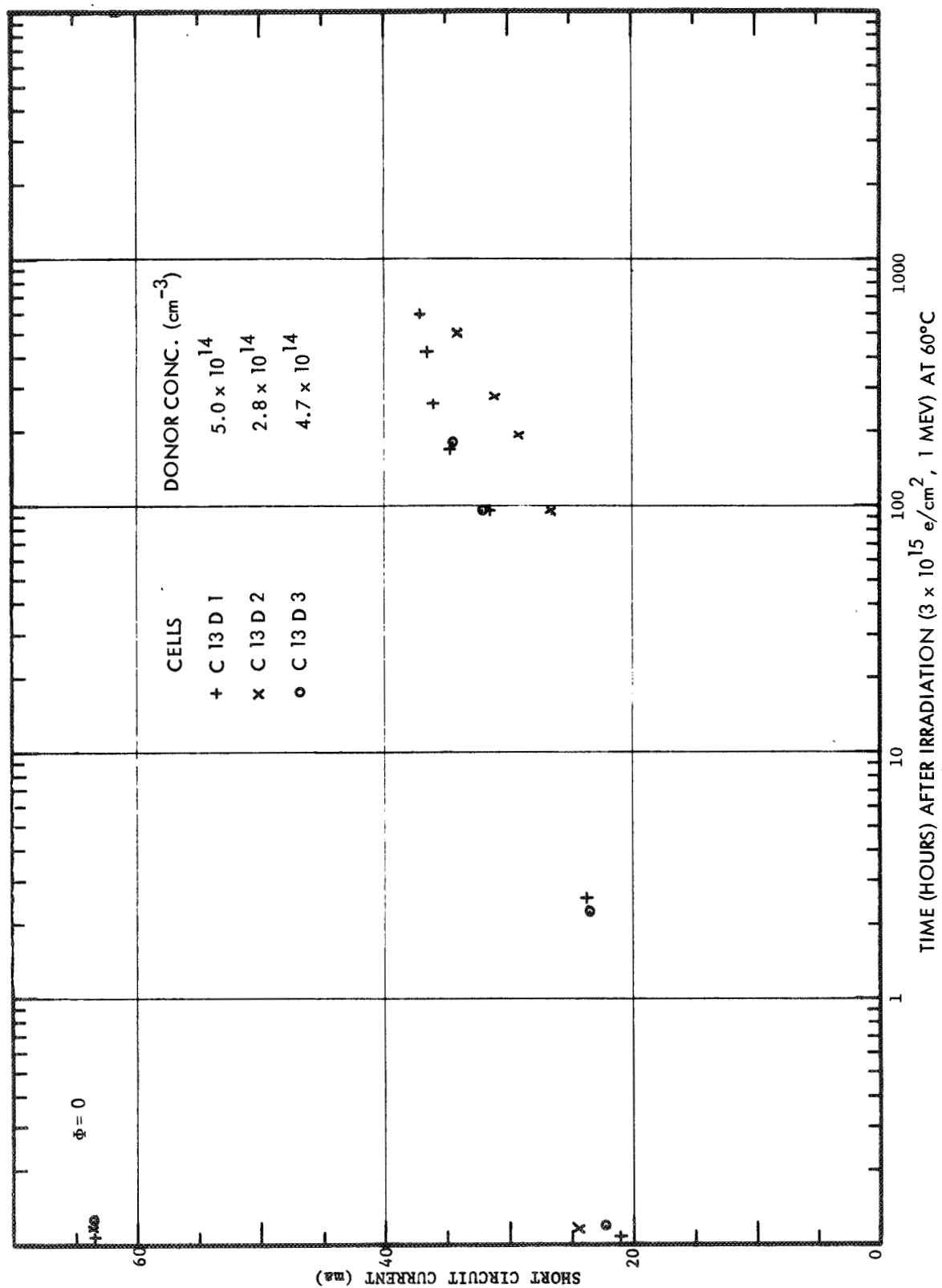


Figure 14. Short Circuit Current During Recovery, Q.C. Cell

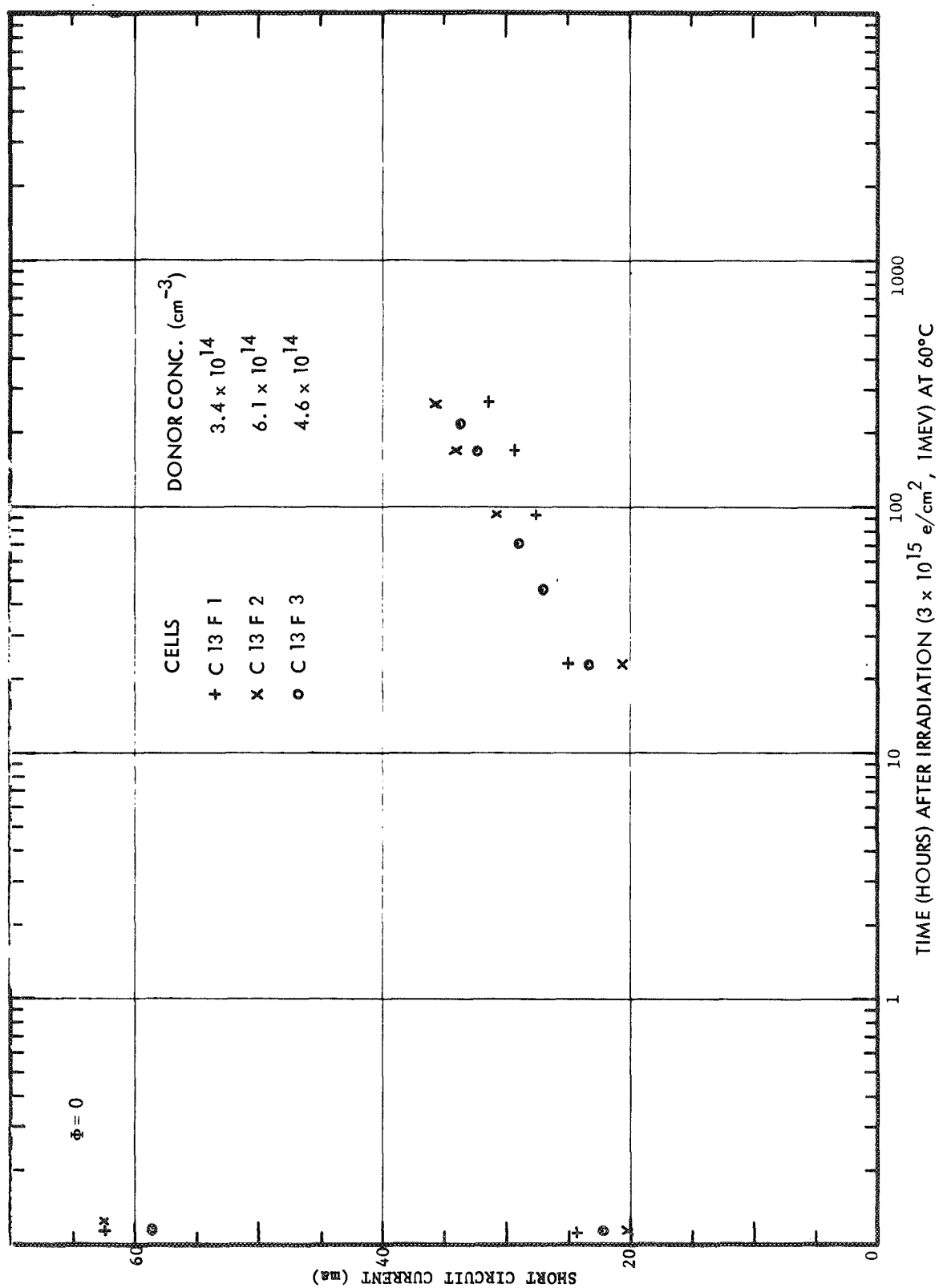


Figure 15. Short Circuit Current During Recovery, Q.C. Cell

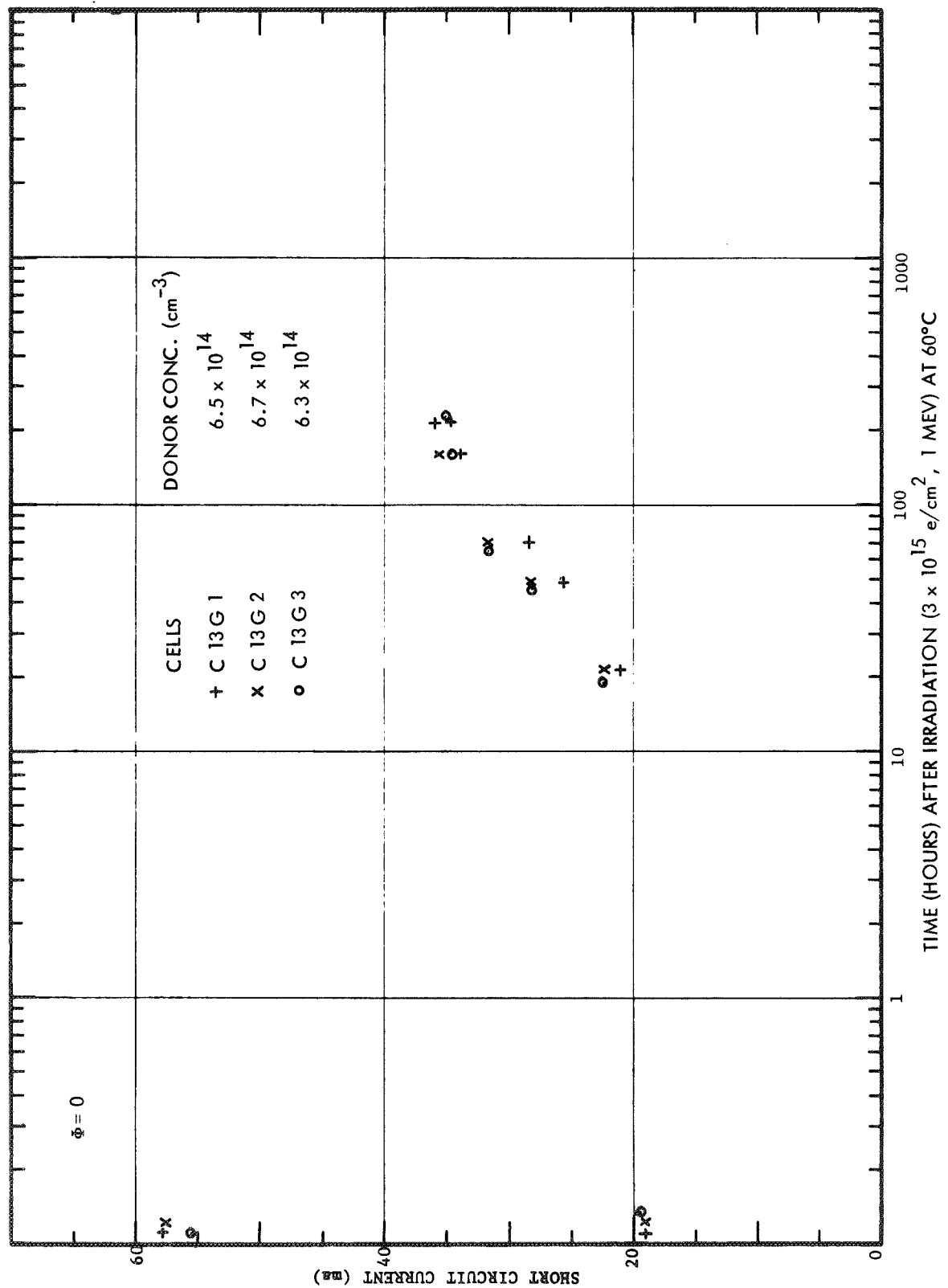


Figure 16. Short Circuit Current During Recovery, Q.C. Cell

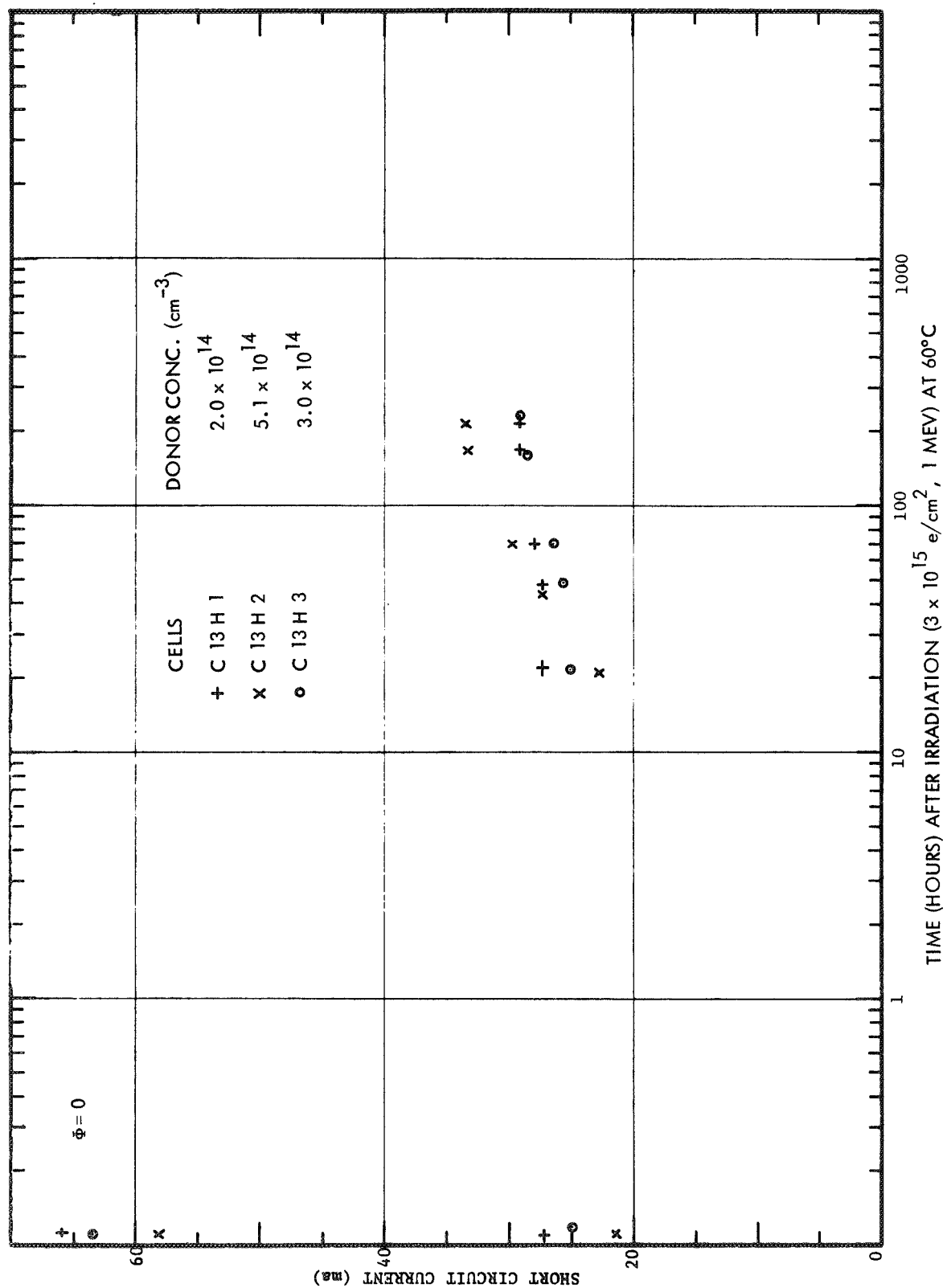


Figure 17. Short Circuit Current During Recovery, Q.C. Cell

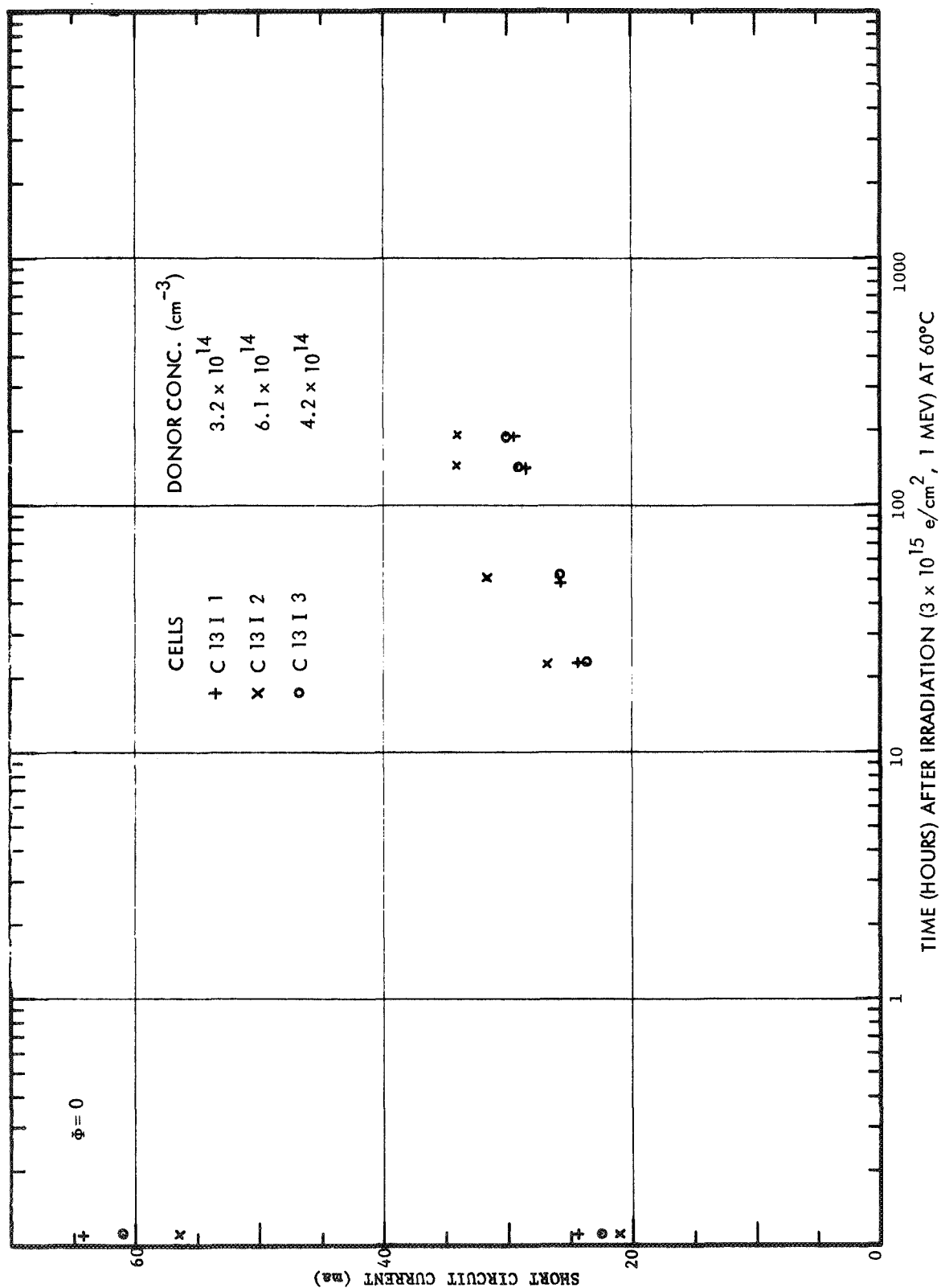


Figure 18. Short Circuit Current During Recovery, Q.C. Cell

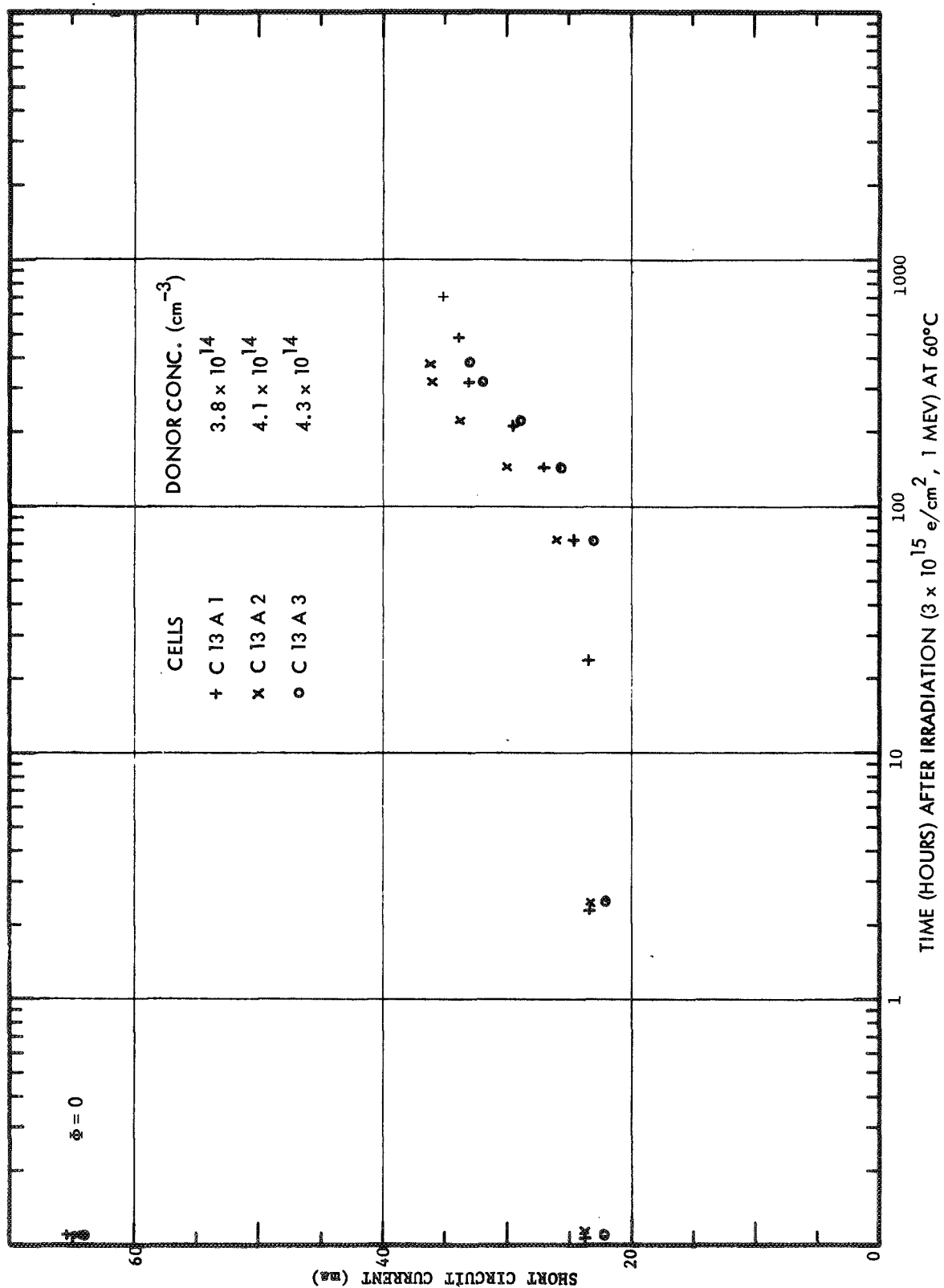


Figure 19. Short Circuit Current During Recovery, Q.C. Cell

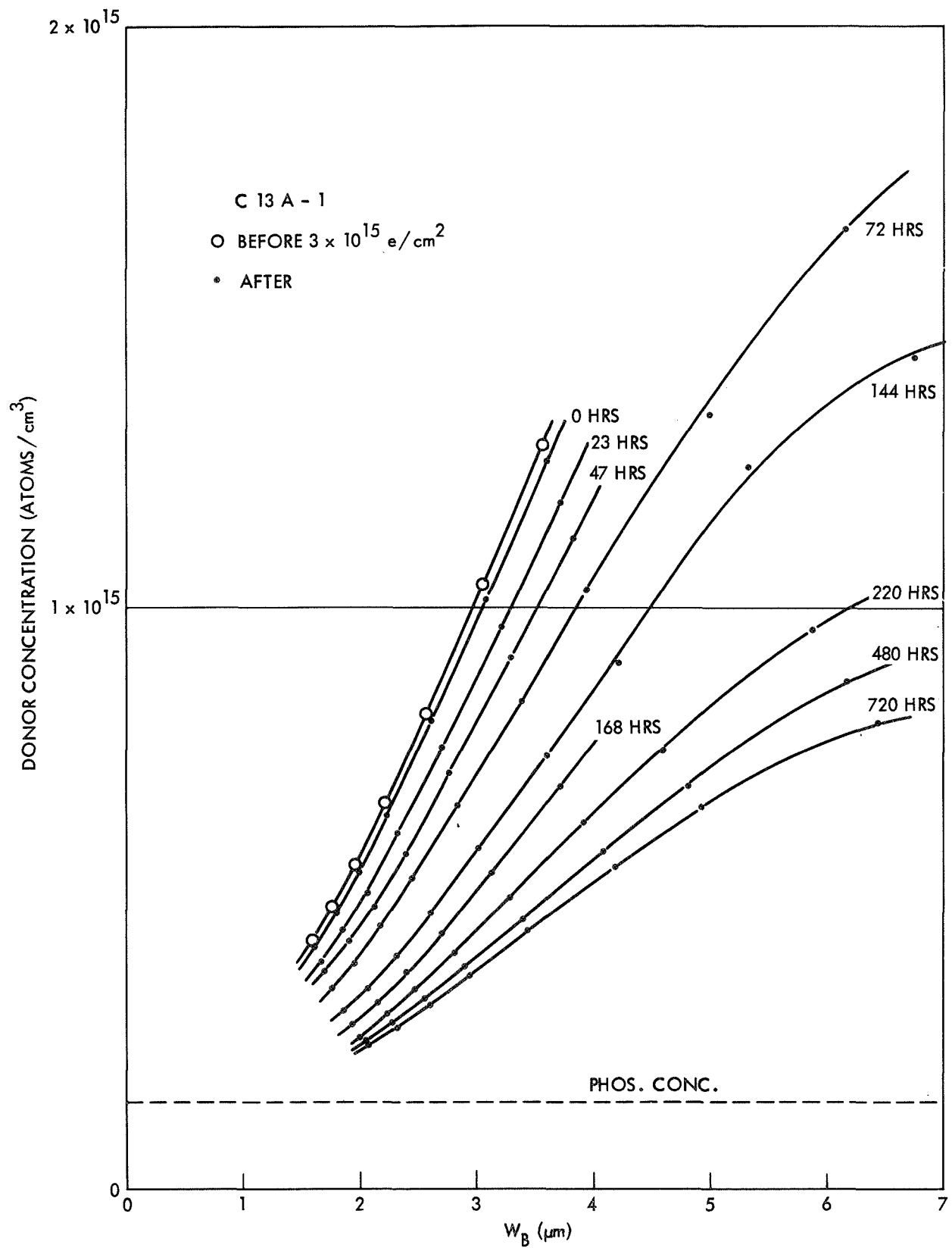


Figure 20. Donor Concentration During Recovery, C13A-1

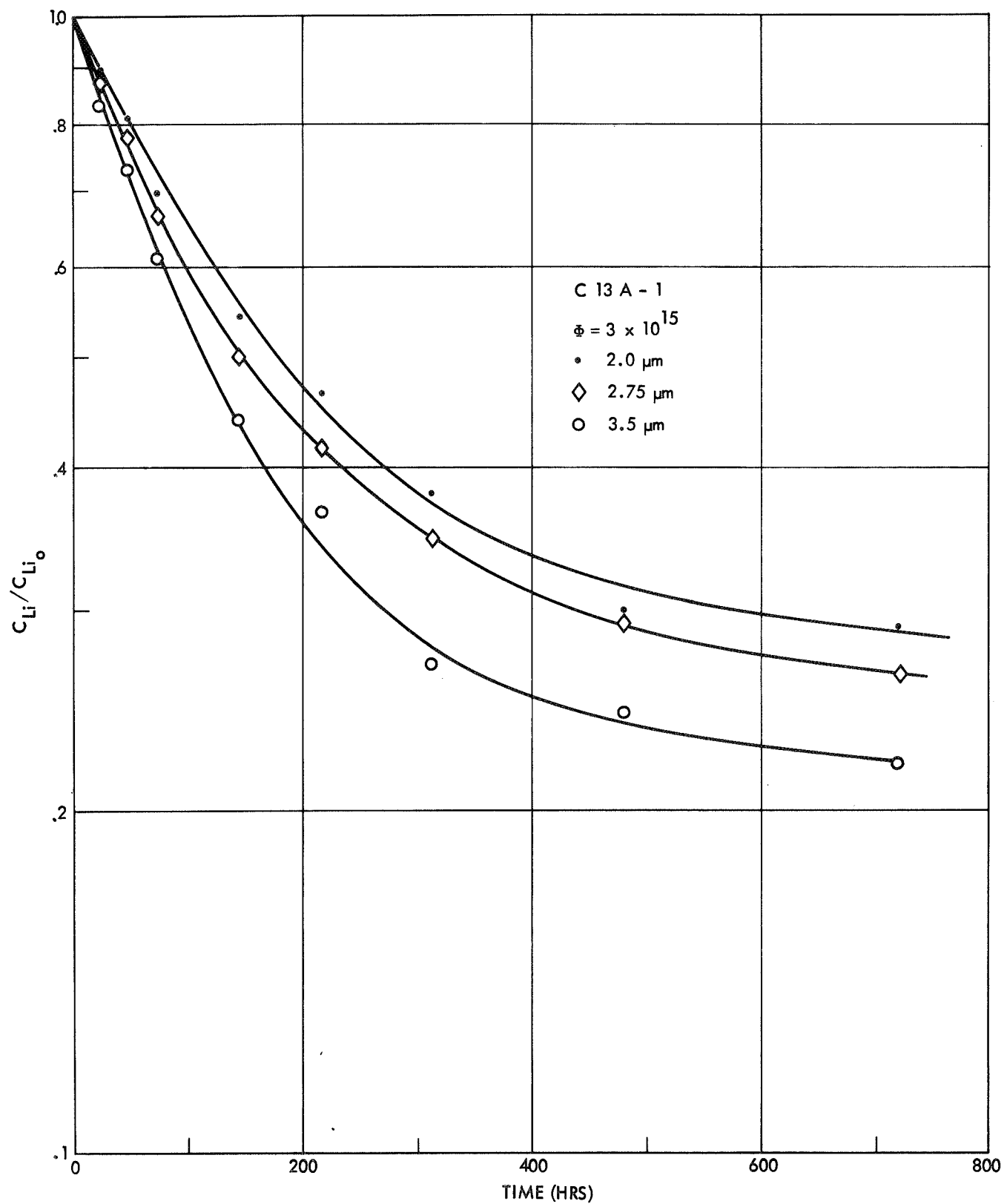


Figure 21. Change in Lithium Donor Concentration During Recovery, C13A-1

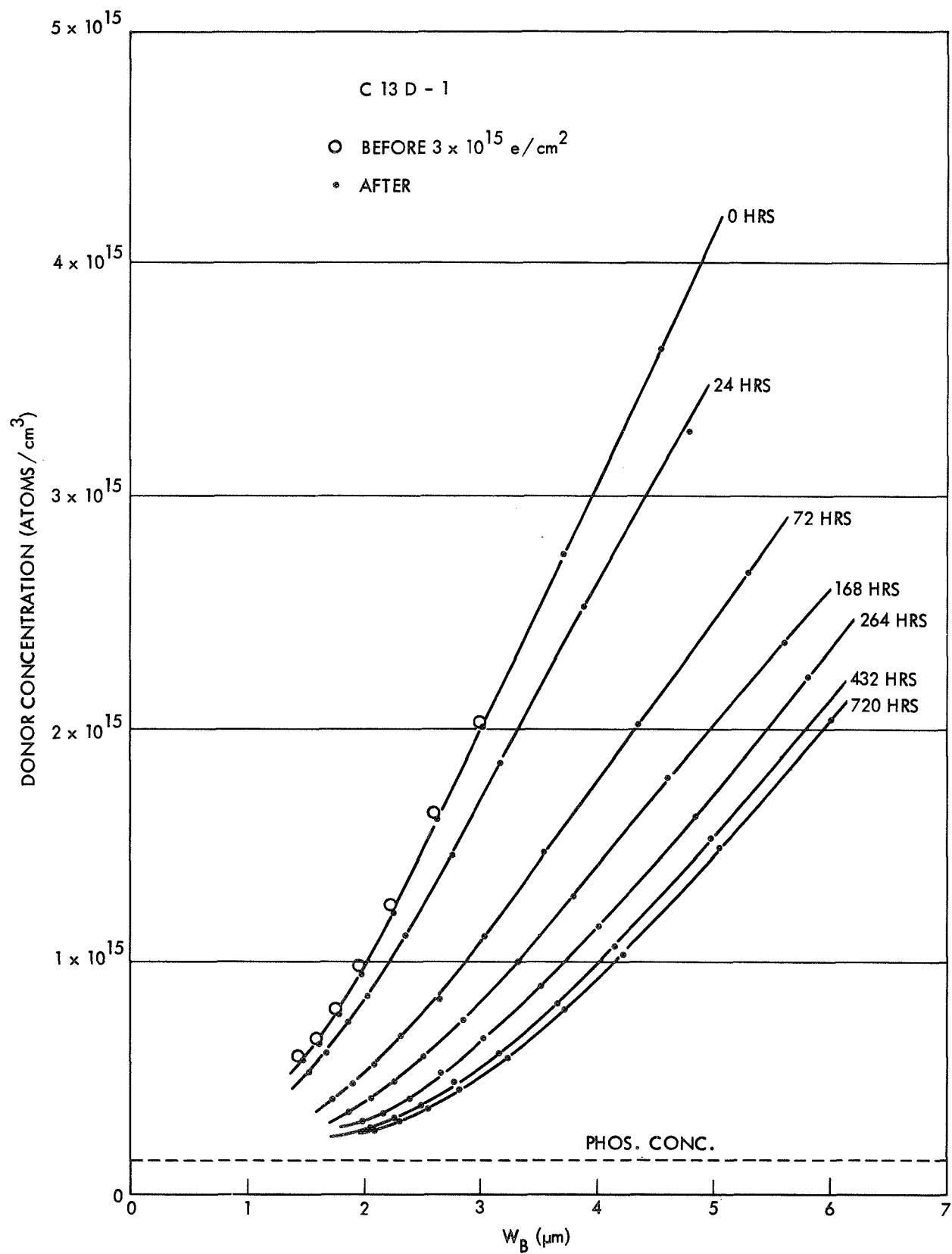


Figure 22. Donor Concentration During Recovery, C13D-1

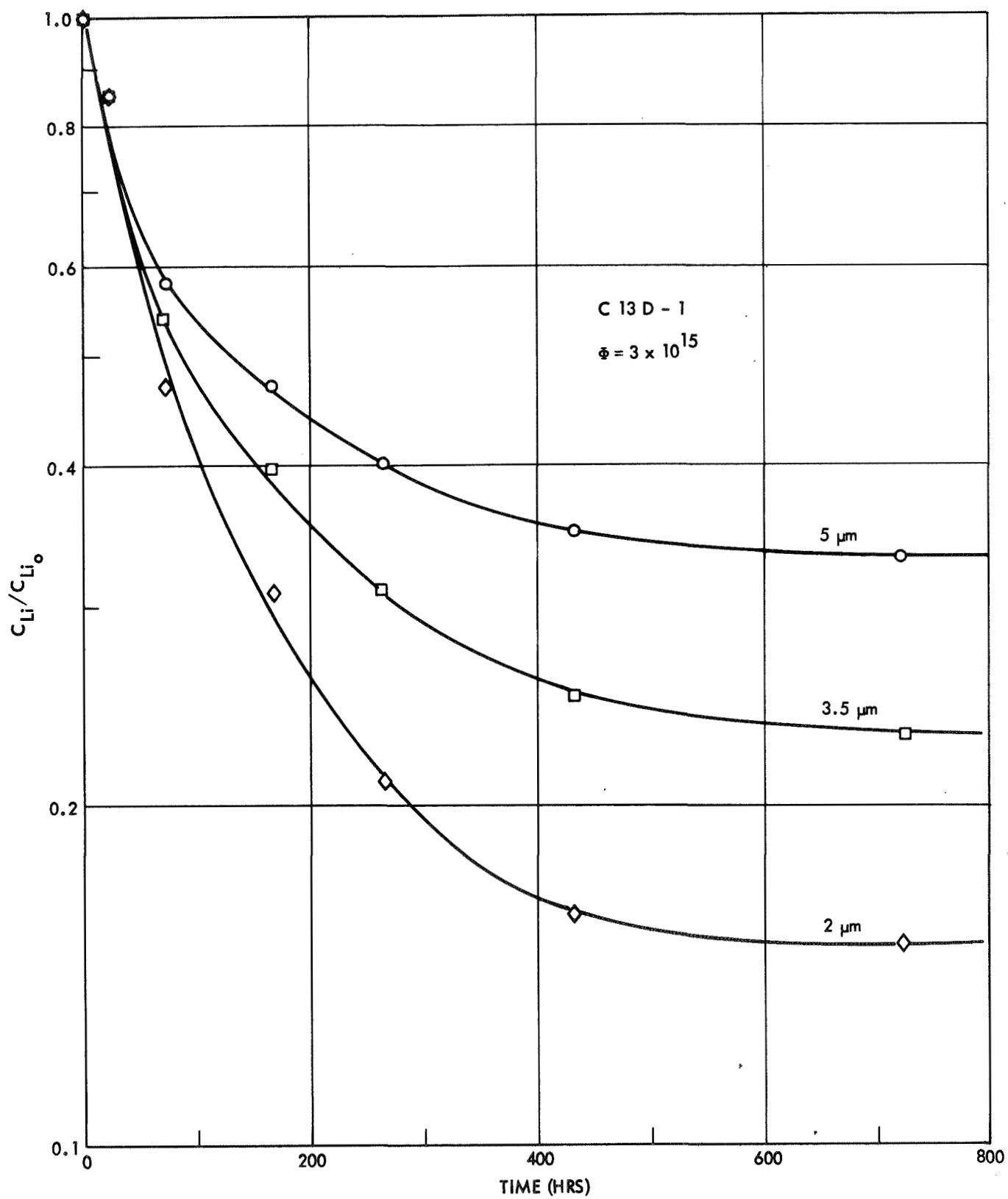


Figure 23. Change in Lithium Donor Concentration During Recovery, C13D-1